ELSEVIER

Journal of Nuclear Materials 277 (2000) 106–112

journal of nuclear materials

www.elsevier.nl/locate/jnucmat

Thermal studies on alkaline earth uranates

S.K. Sali, S. Sampath, V. Venugopal*

Fuel Chemistry Division, Bhabha Atomic Research Centre, Trombay, Mumbai 400085, India

Received 17 February 1999; accepted 1 June 1999

Abstract

The thermal stabilities of various alkaline earth uranates were investigated by thermogravimetry and X-ray powder diffraction. New uranates with the formal composition $A_2U_3O_9$ (A = Ca, Sr and Ba) having hexagonal unit cell were obtained and characterised. Oxidation of these uranates led to the formation of two new intermediate compounds of composition $A_2U_3O_{10}$ (A = Ca and Sr). Many of the calcium and strontium uranates were found to be structurally related to fluorite as long as the substitution of uranium by calcium or strontium was limited to 0.33 and the ratio of oxygen to metal was close to 2. Kinetic studies on the oxidation and the reduction of uranates showed that the oxidation kinetics of $A_2U_3O_9$ to $A_2U_3O_{10}$ (A = Ca, Sr) or $A_2U_3O_{11}$ (A = Ba) was controlled by nucleation and growth whereas the reduction kinetics of $A_2U_3O_{11}$ to $A_2U_3O_9$ (A = Ca, Sr and Ba), generally occurring in single step, was controlled by phase boundaries. © 2000 Elsevier Science B.V. All rights reserved.

1. Introduction

The study of the alkaline earth-uranium-oxygen system is important since Ba and Sr are major fission products and the oxides of the fission products barium, strontium, molybdenum, zirconium and rare earths may either form a solid solution among themselves along with UO_2 or form separate phases in the fuel matrix. Studies on chemical state of fission products in oxide fuels have shown that it is controlled by fission product concentration, O/M ratio and temperature. Quantitative X-ray microanalysis performed on multi component oxide phases of irradiated nuclear fuel has been reported to give compositions such as $(Ba_{1-x-y}Sr_xCs_y)$ (U,Pu,Zr,Mo,RE)O_3 (RE = rare earths) [1].

Among the hexavalent uranates of alkaline earth elements, $A_2U_3O_{11}$ (A = Ba, Sr and Ca) are reported to be the stablest of the uranates in air [2]. AUO_3, $A_2U_2O_7$, AU_2O_6 and AUO_{4-x} are the significant lower valent uranates [3–6]. Apart from these, $A_xU_{1-x}O_{2+y}$ solid solution ($x = 0$–0.30 for Sr and $x = 0$–0.33 for Ca) is also known where divalent alkaline earth metal substitutes for uranium of UO_2 structure [7,8]. The various polyuranates of alkaline earth metals show marked difference in their thermal stabilities in different atmospheres. Literature on thermal stabilities of alkaline earth uranates at elevated temperatures in reducing atmosphere is limited. Most important data are available for the monouranates, AUO_4, which form series of oxygen deficient compounds of the type AUO_{4-x} with both Ca and Sr [9,10]. The reactivity of alkaline earth monouranates with hydrogen is reported to decrease in the following order [9]:

$$\alpha\text{-}SrUO_4 > CaUO_4 > \beta - SrUO_4 > BaUO_4$$

Perovskite-type $A_2UO_{4.5}$ (A = Ca and Sr) compounds have been reported by reduction of A_2UO_5 [11,12]. $BaUO_3$ has been reportedly obtained by reduction of $BaUO_4$ in H_2 at 1673 K and solid solution of the type $BaU_{1-y}Th_yO_3$ has been reported [13]. No literature is available on kinetics of formation of the alkaline earth uranates except on the oxidation of decomposition products of the alkaline earth diuranates [3].

In this paper, the studies on the thermal behavior in hydrogen atmosphere on some of the hexavalent uranates, such as $A_2U_3O_{11}$ (A = Ba, Sr and Ca) and AU_4O_{13} (A = Sr and Ca) are reported. Reduction kinetics of

---

* Corresponding author.

E-mail address: kdsingh@apsara.barc.ernet.in (V. Venugopal).

PII: S0022-3115(99)00145-2

$A_2U_3O_{11}$ in reducing atmosphere and oxidation kinetics of reduced phases in dry air by non-isothermal method are also reported. New uranates $Ba_2U_3O_9$, $Sr_2U_3O_9$, $Sr_2U_3O_{10}$, $Ca_2U_3O_9$ and $Ca_2U_3O_{10}$ have been identified and characterised. X-ray photoelectron spectroscopic studies on some of these compositions namely $Sr_2U_3O_9$, $Sr_2U_3O_{10}$ and $Ba_2U_3O_9$ have been reported by us earlier [14].

2. Experimental

Starting materials for the preparation of AUO_4, $A_2U_3O_{11}$ (A = Ba, Sr and Ca) and AU_4O_{13} (A = Sr and Ca) were A.R. grade ACO_3 and U_3O_8 (nuclear grade). Appropriate proportion of the metal carbonate was mixed with U_3O_8 so as to get the desired M/U ratio. About two grams of this mixture was thoroughly mixed with a small amount of ethyl alcohol, dried and pressed into pellet using hydraulic press with pressure of 5 tons/inch^2. The pellet was calcined at 1100 K in air for 20–30 h with intermittent cooling, crushing, mixing and pressing to make sure of homogeneity. X-ray powder diffraction analysis confirmed the formation of the pure compound. The compounds obtained in this way were subjected to reduction kinetics in flowing Ar + 7%H_2 gas atmosphere at a rate of 2 K/min in the Ulvac thermoanalyser with a balance precision ±0.1 mg. For a sample weight of around 100 mgs, there is a possible error of ±0.1% in the experimental weight losses and gains. UV spectra of the products dissolved in 1M sulphuric acid were recorded on a Beckmann model DU-7 spectrophotometer. Oxidation of these samples were carried out in dry air. The thermoanalyser was calibrated from the weight loss obtained for decomposition of $CaC_2O_4 \cdot H_2O$ to CaO during heating to 1200 K. The calculated and observed weight loss values were in good agreement indicating the reliability of the measurement. X-ray powder patterns were obtained with Diano X-ray diffractometer ($\lambda = 0.154178$ nm) after quenching the samples to room temperature.

3. Results and discussion

Thermogravimetric (TG) curves of $A_2U_3O_{11}$ (A = Ca, Sr and Ba) heated in Ar + 7% H_2 atmosphere are shown as % weight loss versus temperature in Fig. 1. The reduced products were found to be black in colour indicating lower valency of uranium. The curves show that $A_2U_3O_{11}$-type compounds lose weight in a single step in the temperature range 650–950 K. The weight loss of $Ca_2U_3O_{11}$ began at 600 K and was completed at 900 K with a weight loss of 3.5%. Reduction of $Sr_2U_3O_{11}$ and $Ba_2U_3O_{11}$ started at a higher temperature of 750 K and completed at 950 K. The observed weight losses for $Sr_2U_3O_{11}$ and $Ba_2U_3O_{11}$ were 3.05% and 2.95%, respectively. The absorption spectra of the black products dissolved in 1M H_2SO_4 showed absorption peaks corresponding to both U^{IV} and U^{VI} indicating lower valency of uranium in these compounds. U^{V} if present in the compound is known to disproportionate into equal amounts of U^{IV} and U^{VI} in dilute acids.

Expected weight losses for the reactions:

$$Ca_2U_3O_{11} + 2H_2 \rightarrow Ca_2U_3O_9 + 2H_2O \qquad (1)$$

$$Sr_2U_3O_{11} + 2H_2 \rightarrow Sr_2U_3O_9 + 2H_2O \qquad (2)$$

$$Ba_2U_3O_{11} + 2H_2 \rightarrow Ba_2U_3O_9 + 2H_2O. \qquad (3)$$

Eqs. (1)–(3), respectively, should be 3.3%, 3.0% and 2.7%. The weight losses were associated with exothermic DTA peaks. The X-ray powder patterns of the reduced phases were different from any of the reported phases of Ca–U–O, Sr–U–O and Ba–U–O systems. The possibility of a non-cubic phase has been mentioned in the literature for the composition $Sr_{0.4}U_{0.6}O_{2+x}$ during the study of phase relation and crystal chemistry of the solid solution, $Sr_yU_{1-y}O_{2+x}$ [8].

Oxidation of all these $A_2U_3O_9$ (A = Ca, Sr and Ba) type of compounds started at very low temperature (≈373 K) indicating poor thermal stability in air. It has been reported in the literature that alkaline earth monouranates, AUO_{4-x}, which were formed by the hydrogen reduction of stoichiometric monouranates, gradually took up oxygen into the crystal lattice even at room temperature when exposed to air: $CaUO_{3.50}$ to $CaUO_{3.69}$, $SrUO_{3.48}$ to $SrUO_{3.69}$ and $BaUO_{3.50}$ to $BaUO_{3.65}$ [6]. Fig. 2 shows TG of $A_2U_3O_9$ (A = Ca, Sr and Ba) in air. The TG of $A_2U_3O_9$ was carried out in air immediately after the reduction to eliminate chances of oxidation during storing at room temperature. Oxidation of $Ca_2U_3O_9$ started at 325 K and was complete at 1225 K with a weight gain of 3.26%, forming the orange

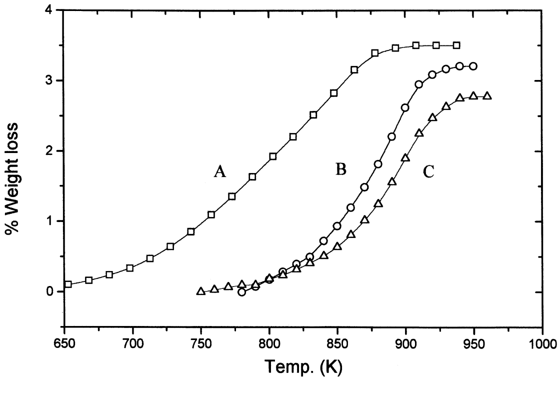

Fig. 1. TG curves for reduction of (A) $Ca_2U_3O_{11}$, (B) $Sr_2U_3O_{11}$ and (C) $Ba_2U_3O_{11}$ in Ar + 7% H_2: heating rate, 2 K/min.

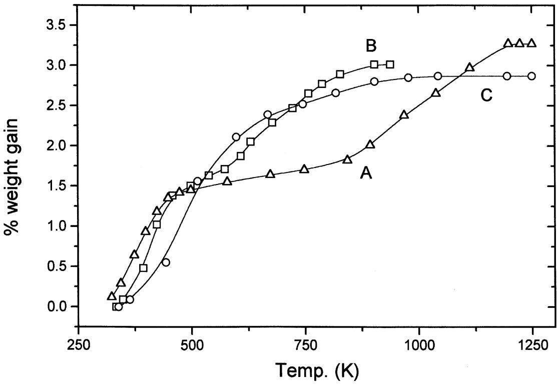

Fig. 2. TG curves for oxidation of (A) $Ca_2U_3O_9$, (B) $Sr_2U_3O_9$ and (C) $Ba_2U_3O_9$ in dry air: heating rate, 2 K/min.

coloured $Ca_2U_3O_{11}$ as the final product as determined by XRD. This oxidation proceeded through an intermediate step corresponding to a weight gain of 1.6% up to 673 K (with a product having greenish black colour) and gain of 1.66% in the second step up to 1273 K. The oxidation reactions can be written as

$$Ca_2U_3O_9 + \frac{1}{2}O_2 \rightarrow Ca_2U_3O_{10} \quad (4)$$

$$Ca_2U_3O_{10} + \frac{1}{2}O_2 \rightarrow Ca_2U_3O_{11}. \quad (5)$$

The theoretical weight gains for reactions 4 and 5 are 1.7% and 1.67%, respectively. The observed and calculated weight gains agreed for the above reactions. Similarly TG of $Sr_2U_3O_9$ in air showed oxidation in two stages with an intermediate step at 525 K and a weight gain of 1.5% giving greenish black compound and the oxidation was complete at 873 K with total weight gain of 3.0% giving orange product. The oxidized phase was determined to be $Sr_2U_3O_{11}$ from XRD. The reaction scheme follows the equations

$$Sr_2U_3O_9 + \frac{1}{2}O_2 \rightarrow Sr_2U_3O_{10} \quad (6)$$

$$Sr_2U_3O_{10} + \frac{1}{2}O_2 \rightarrow Sr_2U_3O_{11} \quad (7)$$

The expected weight gain for reactions 6 and 7 above are 1.55% and 1.52%, respectively. X-ray diffraction patterns of the intermediate products with the compositions $Ca_2U_3O_{10}$ and $Sr_2U_3O_{10}$, were similar to $Ca_2U_3O_9$ and $Sr_2U_3O_9$ patterns respectively, except for a definite shift in line position to higher angle. Oxidation of $Ba_2U_3O_9$ on the other hand took place in single step with a weight gain of 2.95% forming orange coloured $Ba_2U_3O_{11}$ as final product. The oxidation occurred in the temperature range 330–1073 K with a broad exothermic DTA peak. So the reaction can be written as

$$Ba_2U_3O_9 + O_2 \rightarrow Ba_2U_3O_{11}. \quad (8)$$

The expected weight gain for the above oxidation is 2.83%.

All the calculated (and experimental) weight losses and weight gains have been obtained as % losses or % gains of the starting compositions. Thus, the weight gain % refer to % gain on $Ba_2U_3O_9$, $Sr_2U_3O_9$ and $Ca_2U_3O_9$ whereas the weight loss % refer to % loss on $Ba_2U_3O_{11}$, $Sr_2U_3O_{11}$ and $Ca_2U_3O_{11}$.

The XRD pattern of $Sr_2U_3O_9$ and $Sr_2U_3O_{10}$ could be indexed into hexagonal system with lattice parameters $a = 0.3937(1)$ nm, $c = 1.8628(17)$ nm and $a = 0.3921(1)$ nm, $c = 1.8529(7)$ nm, respectively. Similarly $Ca_2U_3O_9$ and $Ca_2U_3O_{10}$ could be indexed into hexagonal systems with lattice parameters $a = 0.3911(2)$ nm, $c = 1.8125(15)$ nm and $a = 0.3874(3)$ nm, $c = 1.7912(14)$ nm, respectively. With the addition of extra oxygen in the lattice of $Ca_2U_3O_9$ and $Sr_2U_3O_9$, both a and c axes parameters decrease indicating contraction of unit cell associated with the oxidation of uranium. $Ba_2U_3O_9$ could also be indexed into hexagonal system with lattice parameters $a = 0.8079(1)$ nm, $c = 1.9512(7)$ nm. The XRD data of the new calcium uranates, $Ca_2U_3O_9$ and $Ca_2U_3O_{10}$, the strontium uranates, $Sr_2U_3O_9$ and $Sr_2U_3O_{10}$ and the barium uranate, $Ba_2U_3O_9$ are given respectively in Tables 1–3. The structures of all the $A_2U_3O_9$-type compounds are similar to that of $Tl_2U_3O_9$ reported earlier [15] [$Tl_2U_3O_9$: Hexagonal: $a = 0.3972(4)$ nm, $c = 0.9960(2)$ nm].

The compounds $Ba_2U_3O_9$, $Sr_2U_3O_9$ and $Ca_2U_3O_9$ could be represented as $M_2U^{IV}U^{V}_{2}O_9$ or $M_2U^{IV}_{2}U^{VI}O_9$ (M = Ba, Sr or Ca). Similarly $Sr_2U_3O_{10}$ and $Ca_2U_3O_{10}$ could be represented as $M_2U^{V}_{2}U^{VI}O_{10}$ or $M_2U^{IV}U^{VI}_{2}O_{10}$ (M = Sr or Ca). XPS measurements reported earlier on some of these compounds showed the dominance of U^V in $Sr_2U_3O_{10}$. Similarly XPS data on $Sr_2U_3O_9$ and $Ba_2U_3O_9$ showed the presence of IV and VI states of U in these compounds. Hence the representation $M_2U^{IV}_{2}U^{VI}O_9$ (M = Ba, Sr or Ca) and $M_2U^{V}_{2}U^{VI}O_{10}$ are more likely to be correct [14].

In the Sr–U–O and Ca–U–O systems, a series of oxygen- deficient monouranates were reported with compositions $SrUO_{3.948}$, $SrUO_{3.777}$, $SrUO_{3.597}$ [16], $CaUO_{3.55}$ and $CaUO_{3.50}$ [17] whose structures are similar to those of $SrUO_4$ and $CaUO_4$ and also to $Sr_2U_3O_9$ and $Ca_2U_3O_9$ presently identified. XRD patterns of a synthetic mixture of $SrUO_{4-x}$ and UO_2 in ratio 2:1 showed distinct lines of UO_2 which were absent in the XRD trace of $Sr_2U_3O_9$ thus confirming the atomic ratio of U/Sr in the new compound as 1.5. These observations showed that $Sr_2U_3O_9$ was different from monouranate, $SrUO_4$ or $SrUO_{4-x}$. Similar observations were noted for $Ca_2U_3O_9$.

Table 1
X-ray powder data on $Ca_2U_3O_9$ and $Ca_2U_3O_{10}$ ($\lambda = 0.154178$ nm)

h	*k*	*l*	$d_{obs.}$	$d_{cal.}$	I/I_0	*h*	*k*	*l*	$d_{obs.}$	$d_{cal.}$	I/I_0
$Ca_2U_3O_9$ (hexagonal, $a = 0.3911$ (2) nm, $c = 1.8125$ (15) nm)						$Ca_2U_3O_{10}$ (hexagonal, $a = 0.3874$ (3) nm, $c = 1.7912$ (14) nm)					
0	0	3	0.6051	0.6042	18	0	0	3	0.5985	0.5971	15
1	0	1	0.3337	0.3329	18	1	0	1	0.3309	0.3297	11
0	1	2	0.3177	0.3172	100	0	1	2	0.3145	0.3143	100
0	0	6	0.3020	0.3021	36	0	0	6	0.2985	0.2985	31
1	0	4	0.2713	0.2713	54	1	0	4	0.2685	0.2685	46
0	1	5	0.2479	0.2475	7	0	1	5	0.2454	0.2449	6
1	0	7	0.2053	0.2057	8						
1	1	0	0.1957	0.1955	26	1	1	0	0.1936	0.1937	32
0	1	8	0.1881	0.1883	29	0	1	8	0.1859	0.1862	22
2	0	2	0.1662	0.1665	13	2	0	2	0.1649	0.1649	13
1	1	6	0.1642	0.1642	27	1	1	6	0.1624	0.1625	27
0	2	4	0.1589	0.1586	16	0	2	4	0.1573	0.1571	13
2	0	8	0.1354	0.1356	7	2	0	8	0.1343	0.1343	8
1	2	2	0.1265	0.1267	6	1	2	2	0.1257	0.1256	8
2	1	4	0.1230	0.1232	6	2	1	4	0.1220	0.1220	7
1	1	12	0.1197	0.1195	9	1	1	12	0.1182	0.1183	6
1	2	8	0.1112	0.1114	7	1	2	8	0.1101	0.1103	8

Table 2
X-ray powder data on $Sr_2U_3O_9$ and $Sr_2U_3O_{10}$

h	*k*	*l*	$d_{obs.}$	$d_{cal.}$	I/I_0	*h*	*k*	*l*	$d_{obs.}$	$d_{cal.}$	I/I_0
$Sr_2U_3O_9$ (hexagonal, $a = 0.3937$ (1) nm, $c = 1.8628$ (17) nm)						$Sr_2U_3O_{10}$ (hexagonal, $a = 0.3921$ (1) nm, $c = 1.8529$ (7) nm)					
0	0	3	0.6202	0.6209	16	0	0	3	0.6207	0.6176	13
1	0	0	0.3410	0.3409	10	1	0	1	0.3358	0.3341	14
1	0	2	0.3202	0.3202	100	0	1	2	0.3194	0.3189	100
0	0	6	0.3102	0.3104	52	0	0	6	0.3092	0.3088	33
1	0	4	0.2751	0.2751	47	1	0	4	0.2742	0.2739	51
1	1	0	0.1968	0.1968	20	1	1	0	0.1961	0.1960	27
1	0	8	0.1922	0.1922	30	0	1	8	0.1916	0.1913	28
1	1	6	0.1662	0.1662	21	1	1	6	0.1655	0.1655	24
1	0	10	0.1634	0.1635	14	1	0	10	0.1627	0.1627	14
2	0	4	0.1601	0.1601	9	0	2	4	0.1596	0.1594	9
2	0	8	0.1373	0.1375	9	2	0	8	0.1369	0.1369	8
2	0	14	0.1238	0.1239	6	1	2	2	0.1269	0.1271	8
1	1	12	0.1220	0.1219	8	0	1	14	0.1235	0.1233	9
2	1	8	0.1125	0.1127	5	1	1	12	0.1214	0.1213	8
2	1	0	0.1056	0.1059	4	1	2	8	0.1123	0.1123	6

Fig. 3 shows TG, in Ar + 7% H_2 atmosphere, of $BaUO_4$, β-$SrUO_4$ and SrU_4O_{13}. The reduction of $BaUO_4$ occurred at higher temperature than that of β-$SrUO_4$. The compound obtained after heating $BaUO_4$ in Ar + 7% H_2 at 1473 K was found by X-ray powder diffraction to be $Ba_2U_2O_7$. However the weight loss was considerably more than expected. Black deposits were noticed on the crucible holder indicating some volatalisation of Ba which could be responsible for the higher weight loss. The compound $Ba_2U_2O_7$ has been reported in literature and was obtained by heating a mixture of Ba_3UO_6, $BaUO_4$ and UO_2 in the ratio 1:1:2 in the temperature range of 973 to 1273 K in oxygen-free argon atmosphere [5]. Stoichiometric $BaUO_3$ was difficult to obtain by reduction of $BaUO_4$. However, when it was heated in dry H_2 at 1473 K for 50 h, it could be prepared. The weight loss of β-$SrUO_4$ began at 673 K, which was about 100 K lower than the initiation temperature of $BaUO_4$. The reduced phase at 1173 K, gave mainly $SrUO_{3.597}$ and a small amount of $SrUO_3$. Reduction of SrU_4O_{13} in Ar + 7% H_2 started at 773 K and was completed at 1073 K giving the product of composition SrU_4O_{10} with fluorite structure having $a = 0.5470$ nm. It could be represented as $Sr_{0.2}U_{0.8}O_{2.00}$ with an overall uranium valence of 4.5. Similarly, on reduction of CaU_4O_{13}, fcc phase of composition $Ca_{0.2}U_{0.8}O_{2.05}$ was formed with $a = 0.5410$ nm. CaO and SrO are known to form solid solutions with UO_2 with solubility limits of 33 and 30 at.%, respectively.

Table 3
X-ray powder data on $Ba_2U_3O_9$ (hexagonal, $a = 0.8079(1)$ nm, $c = 1.9512(7)$ nm

h	k	l	$d_{obs.}$	$d_{cal.}$	I/I_0
0	0	3	0.6506	0.6504	18
1	1	3	0.3432	0.3431	15
2	0	2	0.3296	0.3293	100
0	0	6	0.3261	0.3262	69
1	1	4	0.3106	0.3111	24
2	0	4	0.2841	0.2843	42
0	3	3	0.2196	0.2195	7
2	2	0	0.2019	0.2020	34
2	2	1	0.2008	0.2009	32
2	1	8	0.1792	0.1793	7
1	0	11	0.1718	0.1719	32
1	1	11	0.1624	0.1624	9
4	0	8	0.1421	0.1421	6
2	1	13	0.1306	0.1305	12
2	2	12	0.1266	0.1267	12
4	2	6	0.1225	0.1225	3
1	5	6	0.1173	0.1172	7
5	1	8	0.1116	0.1117	3
4	2	10	0.1095	0.1095	8

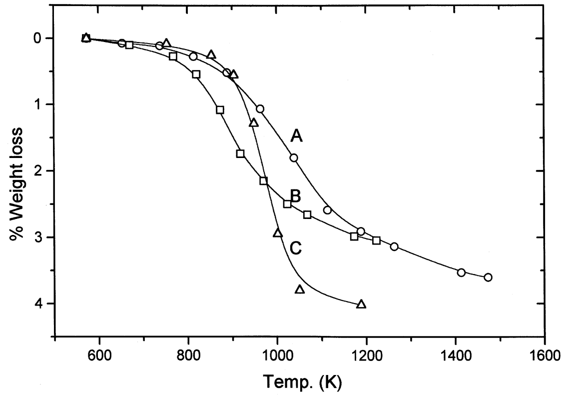

Fig. 3. TG curves for reduction of (A) $BaUO_4$, (B) β-$SrUO_4$ and (C) SrU_4O_{13} in Ar + 7% H_2: heating rate, 2 K/min.

Table 4 gives a summary of data on ternary compounds reported in Sr–U–O system namely, composition, O/M (M = Sr + U), Sr/(Sr + U) ratio and their structures. The composition of all these phases can be represented in the form $Sr_xU_{1-x}O_{2-y}$. When the compounds are arranged with increasing order of their Sr/(Sr + U) ratio and their structures compared, it is found that when $0 < x \leqslant 0.33$ and $0 < y < 0.25$, the structure is fluorite-type. The structure changes to deformed fcc or rhombohedral, when $0.33 \leqslant x \leqslant 0.5$ and $0 \leqslant y \leqslant 0.25$. When $x > 0.5$ and $y > 0.25$, the system can have other than fcc/deformed fcc or rhombohedral structures. Thus in $Sr_xU_{1-x}O_{2-y}$, the structure is fluorite or rhombohedral when $x = 0$–0.5 and $y = 0$–0.25. $CaUO_4$ and $SrUO_4$ (α phase) are reported to be rhombohedral and isostructural. The $CaUO_4$ structure has been regarded by Zachariasen as an appreciably deformed CaF_2 type of structure [18]. The new uranates obtained by us in the Ca–U–O system are isostructural with the corresponding strontium uranates. Thus the above discussion regarding similarities in structure in Sr–U–O system are relevent to Ca–U–O system also. However in Sr–U–O system an orthorhombic phase of $SrUO_4$ (β) has been reported which is stoichiometric and structurally similar to $BaUO_4$ and not related to other strontium or calcium uranates [9].

The structural similarities of many of the uranates in Sr–U–O and Ca–U–O systems can be explained as due to the closeness of crystal radii of Sr^{2+} or Ca^{2+} and U^{4+} and also the ability of UO_2 to have both vacancies and interstitial atoms in its fluorite lattice. This is found to be valid as long as (i) substitution of Sr or Ca for uranium is limited and /or (ii) ratio of oxygen to metal (O/M) remains close to 2. Further substitution of U by Sr or Ca or a large deviation in O/M from 2 leads to major change in structure. The uranates of barium however did not show any structural similarity among themselves or with those of calcium or strontium.

For the purpose of obtaining kinetic data, the fraction α reacted ($= W_T - W_0/(W_\infty - W_0)$, where W_0 is the initial weight, W_T is the weight at temperature T and W_∞ is weight after completion of the reaction) for reduction of $A_2U_3O_{11}$ (A = Ca, Sr or Ba) in Ar + 7% H_2 mixture was obtained for various temperatures from TG curves. XRD of the products obtained at various stages of α between 0.2 and 0.9 indicated the presence of $A_2U_3O_{11}$ and $A_2U_3O_9$. $A_2U_3O_{10}$ was found to be absent. However $A_2U_3O_9$ (A = Ca and Sr) when heated in air gave $A_2U_3O_{10}$ as an intermediate. The procedure followed for obtaining kinetic parameters by non-isothermal thermogravimetry has been reported earlier [19,20]. A typical computer output containing standard deviations for various mechanisms and activation energies for reduction of $Ca_2U_3O_{11}$ in Ar + 7% H_2 is given in Table 5. The lowest standard deviation occurred at an activation energy of 63 kJ mol^{-1}. Further iteration for smaller interval of activation energy was carried out which gave a value of 65 kJ mol^{-1}. Thus the entire course of reduction of $Ca_2U_3O_{11}$ to $Ca_2U_3O_9$ is governed by a phase boundary reaction following the relation, $g(\alpha) = [1 - (1 - \alpha)^{1/3}]$. Similarly the reduction kinetics of $Sr_2U_3O_{11}$ to $Sr_2U_3O_9$ and $Ba_2U_3O_{11}$ to $Ba_2U_3O_9$ followed phase boundary reaction with activation energies of 147 kJ mol^{-1} and 145 kJ mol^{-1}, respectively. Table 6 gives kinetic data of reduction of $A_2U_3O_{11}$ (A = Ca,Sr or Ba) in Ar + 7% H_2. Oxidation kinetics of these reduced phases were carried out in air and the kinetic data of oxidation of $A_2U_3O_9$ in air is given in Table 7.

A comparison of Tables 6 and 7 show that the reduction kinetics of $A_2U_3O_{11}$ to $A_2U_3O_9$ in H_2 is phase

Table 4

Compounds	Composition in the form $Sr_xU_{1-x}O_{2-y}$	O/M	Sr/(Sr + U) (x)	Structure
SrU_4O_{10}	$Sr_{0.2}U_{0.8}O_{2.0}$	2.0	0.2	Fluorite
SrU_2O_6	$Sr_{0.33}U_{0.67}O_{2.0}$	2.0	0.33	Fluorite
$Sr_2U_3O_{10}$	$Sr_{0.4}U_{0.6}O_{2.0}$	2.0	0.4	Rhombohedral (deformed fcc)
$Sr_2U_3O_9$	$Sr_{0.4}U_{0.6}O_{1.8}$	1.8	0.4	
$Sr_2U_3O_{11}$	$Sr_{0.4}U_{0.6}O_{2.2}$	2.2	0.4	
α-$SrUO_4$	$Sr_{0.5}U_{0.5}O_{2.0}$	2.0	0.5	
$SrUO_{3.777}$	$Sr_{0.5}U_{0.5}O_{1.889}$	1.9	0.5	
$SrUO_{3.5}$	$Sr_{0.5}U_{0.5}O_{1.75}$	1.75	0.5	
β-$SrUO_4$	$Sr_{0.5}U_{0.5}O_{2.0}$	2.0	0.5	Orthorhombic
$SrUO_3$	$Sr_{0.5}U_{0.5}O_{1.5}$	1.5	0.5	Orthorhombic
$Sr_2UO_{4.5}$	$Sr_{0.66}U_{0.33}O_{1.5}$	1.5	0.66	Pseudo orthorhombic
Sr_3UO_6	$Sr_{0.75}U_{0.25}O_{1.5}$	1.5	0.75	Monoclinic
Sr_3UO_5	$Sr_{0.75}U_{0.25}O_{1.25}$	1.25	0.75	Orthorhombic

Table 5
Reduction of $Ca_2U_3O_{11}$ in Ar+ 7% H_2: A typical computer output (standard deviation) to find the best fit among the different reaction mechanisms

Mechanisms $g(\alpha) =$	Input activation energies (kJ/mol)						
	47	55	63	72	80	88	97
1. $\alpha^{1/4}$	0.3421	0.4076	0.4729	0.5380	0.6030	0.6679	0.7328
2. $\alpha^{1/3}$	0.3055	0.3701	0.4362	0.5013	0.5663	0.6313	0.6961
3. $\alpha^{1/2}$	0.2328	0.2980	0.3632	0.4282	0.4931	0.5580	0.6228
4. α	0.0463	0.0888	0.1488	0.2118	0.2757	0.3399	0.4043
5. $\alpha^{3/2}$	0.2199	0.1588	0.1032	0.0680	0.0842	0.1341	0.1931
6. α^2	0.4392	0.3752	0.3121	0.2503	0.1909	0.1366	0.0967
7. $1-(1-\alpha)^{1/3}$	0.1463	0.0819	**0.0246**	0.0549	0.1178	0.1822	0.2467
8. $1-(1-\alpha)^{1/2}$	0.1038	0.0420	0.0366	0.0970	0.1610	0.2256	0.2902
9. $-\ln(1-\alpha)^{1/4}$	0.2790	0.3444	0.4097	0.4749	0.5399	0.6048	0.6697
10. $-\ln(1-\alpha)^{1/3}$	0.2214	0.2868	0.3521	0.4172	0.4822	0.5471	0.6119
11. $-\ln(1-\alpha)^{1/2}$	0.1075	0.1722	0.2372	0.3021	0.3670	0.4318	0.4966
12. $-\ln(1-\alpha)^{2/3}$	0.0305	0.0623	0.1240	0.1880	0.2524	0.3170	0.3817
13. $-\ln(1-\alpha)$	0.2454	0.1813	0.1189	0.0631	0.0479	0.0952	0.1557
14. $(1-\alpha)\ln(1-\alpha)+\alpha$	0.5682	0.5031	0.4384	0.3740	0.3100	0.2466	0.1844
15. $1-2\alpha/3-(1-\alpha)^{2/3}$	0.6249	0.5596	0.4946	0.4298	0.3652	0.3010	0.2371
16. $[1-(1-\alpha)^{1/3}]^2$	0.7431	0.6777	0.6125	0.5475	0.4827	0.4180	0.3535
17. $[(1+\alpha)^{1/3}-1]^2$	0.3370	0.2745	0.2141	0.1579	0.1117	0.0922	0.1138
18. $1-(1-\alpha)^2$	0.1820	0.2440	0.3072	0.3701	0.4351	0.4993	0.5637
19. $1-(1-\alpha)^3$	0.2738	0.3377	0.4019	0.4662	0.5306	0.5951	0.6596
20. $1-(1-\alpha)^4$	0.3311	0.3958	0.4605	0.5252	0.5898	0.6545	0.7191

boundary controlled whereas the oxidation kinetics of $A_2U_3O_9$ to $A_2U_3O_{10}$ in air is controlled by nucleation and growth following the relation $g(\alpha) = -\ln\ (1-\alpha)^{3/2}$. The oxidation of $Sr_2U_3O_9$ and $Ca_2U_3O_9$ to $Sr_2U_3O_{10}$ and $Ca_2U_3O_{10}$ is not likely to be controlled by well defined phase boundaries as these structures are similar. The reduction of $Ba_2U_3O_{11}$, $Sr_2U_3O_{11}$ and $Ca_2U_3O_{11}$ in H_2 directly gave $A_2U_3O_9$ with distinct structural changes and hence associated with phase boundaries. However, the kinetics of oxidation of $Ba_2U_3O_9$ to $Ba_2U_3O_{11}$ followed nucleation and growth. No information is available regarding the structure of $Ba_2U_3O_{11}$.

Our results on Sr–U–O system show that the solid solution, $Sr_xU_{1-x}O_{2+y}$ is readily formed and formation of $SrUO_3$ requires higher temperature and lower oxygen potentials. In Ba-U-O system, we could not find any evidence for the existence of solid solution of the type $Ba_xU_{1-x}O_{2+y}$. Hence as far as the chemical state of fission products, Ba and Sr in UO_2 and (U,Pu)O_2 are concerned, literature data and our results indicate that Sr may be predominantly dissolved in UO_2 or (U,Pu)O_2. $SrUO_3$ or Sr(U,Pu)O_3-type phase may be precipitated at relatively lower oxygen potentials and higher temperatures. Ba has negligible solid solubility in UO_2 or

Table 6
Reduction kinetics of $A_2U_3O_{11}$ in Ar+7% H_2 (A = Ca, Sr and Ba) $g(\alpha) = 1 - (1-\alpha)^{1/3}$

Composition		α range	$E \pm 5$ (kJ/mol)	Z (s^{-1})
Initial	Reduced			
$Ca_2U_3O_{11}$	$Ca_2U_3O_9$	0.2–0.9	65	0.29×10
$Sr_2U_3O_{11}$	$Sr_2U_3O_9$	0.2–0.9	147	0.16×10^6
$Ba_2U_3O_{11}$	$Ba_2U_3O_9$	0.2–0.9	145	0.90×10^5

Table 7
Kinetic data for oxidation of $A_2U_3O_9$ in air (M = Ca, Sr, Ba) $g(\alpha) = -\ln(1-\alpha)^{3/2}$ [a]

Composition		α range	Mechanism	$E \pm 5$ (kJ/mol)	Z (s^{-1})
Initial	Oxidized				
$Ca_2U_3O_9$	$Ca_2U_3O_{10}$	0.3–0.9	AE3	12.62	0.36×10^{-1}
$Sr_2U_3O_9$	$Sr_2U_3O_{10}$	0.1–0.9	AE3	9.72	0.33×10^{-2}
$Ba_2U_3O_9$	$Ba_2U_3O_{11}$	0.2–0.9	AE3	13.96	0.97×10^{-2}

[a] AE3 = Avrami–Erofeev nuclei growth.

$(U,Pu)O_2$ and hence may be predominantly present as $BaUO_3$ or $Ba(U,Pu)O_3$.

Acknowledgements

The authors gratefully acknowledge Shri R. Prasad, Head, Fuel Development Chemistry Section and Dr D.S.C. Purushotham, Director Nuclear Fuels group for their constant encouragement during the course of this work.

References

[1] H. Kleykamp, J. Nucl. Mater. 131 (1985) 221.

[2] C. Keller, in: K.W. Bagnall (Ed.), MTP International Review of Science, Inorganic Chemistry Series I, vol. 7, 1972, p. 47.

[3] H.R. Hoekstra, J.J. Katz, J. Am. Chem. Soc. 74 (1952) 1683.

[4] S.A. Barrett, A.J. Jacobson, B.C. Tofield, B.E.F. Fender, Acta Crystallogr. B 38 (1982) 2775.

[5] E.H.P. Cordfunke, D.J.W. Ijdo, J. Phys. Chem. Solids 49 (1988) 551.

[6] T. Yamashita, Report JAERI-1310, 1988.

[7] T. Yamashita, T. Fujino, J. Nucl. Mater. 136 (1985) 117.

[8] T. Fujino, Y. Yamashita, H. Tagawa, J. Solid. State Chem. 73 (1988) 544.

[9] H. Tagawa, T. Fujino, T. Yamashita, J. Inorg. Nucl. Chem. 41 (1979) 1729.

[10] E.H.P. Cordfunke, B.O. Loopstra, J. Inorg. Nucl. Chem. 29 (1967) 51.

[11] J. Holc, D. Kolar, J. Solid State Chem. 47 (1983) 98.

[12] E.H.P. Cordfunke, D.J.W. Ijdo, J. Solid State Chem. 109 (1994) 272.

[13] Y. Hinatsu, J. Solid State Chem. 102 (1993) 566.

[14] S. Bera, S.K. Sali, S. Sampath, S.V. Narasimhan, V. Venugopal, J. Nucl. Mater. 255 (1998) 26.

[15] S.K. Sali, V.S. Iyer, K. Jayanthi, S. Sampath, V. Venugopal, J. Alloys Compounds 237 (1996) 49.

[16] J. Kalima, D. Jakes, J. Moravec, J. Inorg. Nucl. Chem. 28 (1966) 1861.

[17] J.C. Bobo, Rev. Chim. Miner. 1 (1964) 3.

[18] W.H. Zachariasen, Acta Crystallogr. 1 (1948) 281.

[19] P.V. Ravindran, Thermochim. Acta 39 (1980) 135.

[20] S.K. Sali, S. Sampath, V. Venugopal, J. Nucl. Mater. 252 (1998) 131.